Theoretical Study of Iron Porphyrin Imine Specie of P411 Enzyme: Electronic Structure and Regioselectivity of C(sp^3)-H Primary Amination

LI Shuang[a, b] WEN Zi-Hao[b] ZHANG Min-Yi[b①]

[a] (*College of Chemistry, Fuzhou University, Fuzhou* 350108, *China*)

[b] (*Fujian Institute of Research on the Structure of Matter, Chinese Academy of Sciences, Fuzhou* 350002, *China*)

ABSTRACT The cytochrome P411 enzyme is a variant of cytochrome $P450_{BM3}$ from Bacillus megaterium whose active site is an iron porphyrin imine ($[Fe(Por)(NH)]^-$) specie. This specie has been reported to successfully promote the primary amination of benzylic and allylic C(sp^3)−H bonds. We employed density functional theory to study the electronic structure of the active site of P411 enzyme and the primary amination of C−H bond reaction that it catalyzes. The calculated spin densities and orbital values indicate the existence of resonance in this specie; namely, $[(por)(–OH)Fe^{IV}–N^{2-}–H]^- \leftrightarrow [(por)(–OH)Fe^{III}–N^{\bullet-}–H]^-$. The amination of C($sp^3$)−H bonds consists of two main reaction steps: hydrogen-atom abstraction and radical recombination, and the former is demonstrated to be the rate-determining step. Furthermore, we studied the regioselectivity of the amination of primary and secondary C(sp^3)−H bonds. Our calculations indicated that the secondary C(sp^3)−H bonds of the substrate would be more favored for the activation by P411 enzyme. These results provide valuable information for understanding the properties and selectivity of C−H/C−N bond-activation reactions catalyzed by the P411 enzyme or other similar enzymes.

Keywords: DFT, cytochrome P411 enzyme, C–H bond activation, enzyme catalysis;

DOI: 10.14102/j.cnki.0254-5861.2011-3191

1 INTRODUCTION

Nitrogen is one of the basic elements present in all living organisms[1]. The primary amine (NH_2) is an important, nitrogen-containing functional group that serves as an essential intermediate in the construction of secondary amines, tertiary amines, and heterocycles. Primary amines are widely present in FDA-approved, bestselling drugs such as imatinib, meclizine, clopidogrel, sertraline, rivastigmine, and donepezil among many others[2-5]. The traditional synthesis of primary amines is usually achieved by the reduction of azides or nitriles, the reductive amination of carbonyl compounds[6], or the Buchwald-Hartwig amination of aryl halides[7, 8]. Unfortunately, nitrogen cannot be introduced into natural organic molecules by direct activation of their C–H bonds[9-13]. However, this would be a beneficial protocol as it could convert C−H bonds directly into C−N bonds[14-17]. In recent years, C−H functionalization has emerged as a promising strategy for amine synthesis. For instance, the selective and direct installation of new functional groups into the hydrocarbon framework of organic compounds can greatly simplify amine synthesis, thus reducing waste and promoting sustainable chemical production[18-20]. Some progress has been recently made in protocols providing the primary amination of C(sp^2)–H bonds, such as photoredox catalysis[21, 22], electrochemical catalysis[23], and the use of other novel amination reagents and metal catalysts[5, 24-29].

It is well known that enzymes offer numerous advantages to biological catalysis, such as excellent stereoselectivity and high reaction rates. For instance, cytochrome P450 enzymes are hemoproteins that catalyze the hydroxylation of nonactivated C−H bonds with a potentially high degree of stereo- and regioselectivities[30]. However, the primary amination of C(sp^3)–H bonds remains a challenge in biology.

Received 24 March 2021; accepted 8 July 2021

① Corresponding author. E-mail: myzhang@fjirsm.ac.cn

Notably, Arnold and coworkers successfully designed the cytochrome P411 enzyme through the directed evolution of a cytochrome P450 from Bacillus megaterium, $P450_{BM3}$. These engineered, iron-heme enzymes can catalyze benzylic and allylic C(sp^3)−H aminations with excellent reactivity and regioselectivity[31-33]. Recently, Arnold and coworkers were the first to report the primary amination of C−H bonds catalyzed by NH-bearing iron porphyrin (Fe (Por)(NH)) specie of the P411 enzyme, where tetrahydronaphthalene (**1**) and 1-(3-methylphenyl)ethane (**2**)[32] served as the substrates (Scheme 1). In reaction 1, the primary amination of benzylic C−H bond of **1** gives tetrahydronaphthalen-1-amine (**1a**) as the main product and **1b** as a low-yield byproduct. In reaction 2, 1-(3-methylphenyl)ethan-1-amine (**2a**) is the main product reported, indicating that the primary amination of the secondary C(sp^3)–H bond of **2** is more favorable than that of the primary C(sp^3)–H bond[32, 34]. However, the active structure of the P411 enzyme and the reaction mechanism of the primary amination of C−H bonds are still unclear, particularly the regioselectivity of the primary amination of different C−H bonds in a substrate.

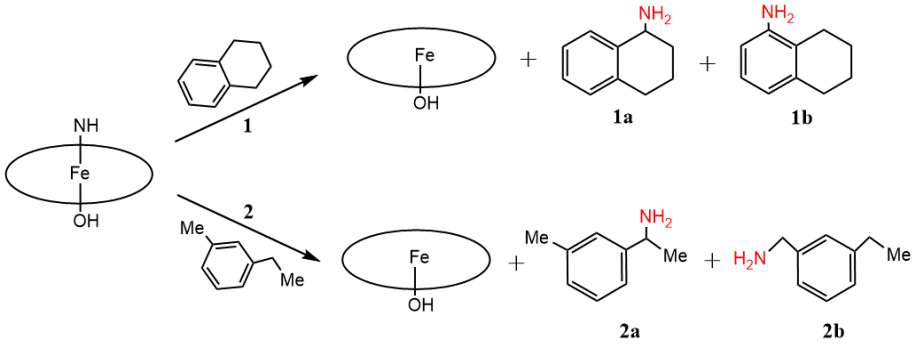

Scheme 1. Primary amination of C−H bonds catalyzed by cytochrome P411 enzyme

In this work, we employed the density functional theory (DFT) method to study the active structure of the cytochrome P411 enzyme and the reaction mechanism of the P411-catalyzed primary amination reactions of substrates **1** and **2**. Furthermore, we revealed the regioselectivity of the mechanism behind the primary amination of the primary and secondary C(sp^3)−H bonds in **2**. The electronic characteristics and geometrical structures of the transition states and intermediates of these aminations were also investigated, and reasonable reaction pathways were elucidated.

2 COMPUTATION METHODS AND DETAILS

2. 1 Setup of the system

According to the relevant literature reported by Arnold[32, 33], we used the crystal structure of the variant closely related to P411-B2 (PDB ID: 5UCW) as the initial structure. All the missing hydrogen atoms in the systems were added by the LEaP program of Amber 20 package. The force field for metal and its surrounding amino acids was parameterized by using "MCPB.py" model[35]. The parameters for residue HEM, -NH and substrate were obtained by the parmchk utility from AMBERTools using the general AMBER force field (gaff)[36]. The protonated states of all titratable residues were determined by the PROPKA program at the experimental optimum pH = 7.4[37], and visually inspected using VMD software[38]. To simulate the enzyme-catalyzed environment, the proteins were immersed in A periodic TIP3P tank with a minimum distance of 15 Å from the protein boundary. Then, several Cl^-/Na^+ ions were added to neutralize the total charges of the systems. The protein in all the simulations were described by the Amber ff14SB force field.

2. 2 MD simulations

After system setup, first, all the water molecules are minimized while keeping the protein fixed, and then the minimization is performed when the whole system is relaxed. Subsequently, the system was gradually heated from 0 to 300 K under the NVT ensemble for 300 ps with a 1 fs time step[39, 40]. This was followed by equilibrating the density of the systems for 1 ns in NPT ensemble at a target temperature of 300 K and pressure of 1.0 atm. During this procedure, Langevin thermostat with collision frequency of 2 ps^{-1} and Berendsen barostat with pressure relaxation time of 1 ps were used to maintain the temperature and density of the system. Thereafter, the system was further equilibrated for 4 ns, followed by a productive MD run of 100 ns for the system[41]. The root-mean-squared deviations (RMSD) of the trajectory were calculated for the MD simulation, as shown in Fig. 1.

We can see that the whole system remains very stable. The QM region in our QM calculations includes Fe, porphyrin ligand, NH group, and the side chains of serine residues Ser398.

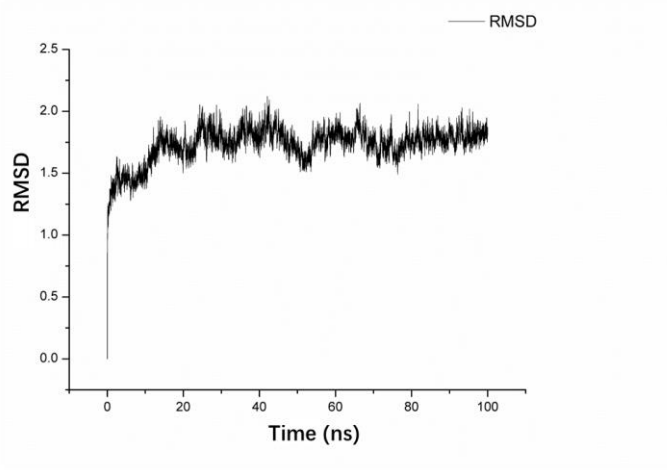

Fig. 1. RMSD analysis of the whole system

2. 3 QM methodology

All calculations were performed using the ORCA 3.0.3 software program and UB3LYP functional[42, 43]. We use the ORCA keyword "BrokenSym" to calculate the open-shell state. All geometric optimizations were performed using the Def2-SVP basis set (BS1). Def2-TZVP basis set (BS2) was used for single-point energy calculations. We use SMD model to calculate the solvent effect to correct the single-point energy[44]. Following the conditions set in previous studies exploring enzyme-catalyzed reactions, the SMD solvation model for chlorobenzene was used to simulate a non-polar protein environment, and the dispersion corrections were computed with Grimme's D3BJ method[43]. For all species, the electronic structure was checked by visualizing spin-natural orbitals (SNOs) at the BS1 level and spin-natural orbitals at the BS2 level.

After geometric optimization, the frequencies of all species were calculated to ensure that all the optimized structures had no imaginary frequencies, and that the transition states had only one imaginary frequency with correct vibration direction, from which the zero-point energy was obtained. Intrinsic reaction coordination (IRC) calculations were performed to confirm the relationships among the transition state, the reactant, and the product. In order to facilitate calculation, the porphyrin ligand was modeled as porphine[45], as has been done in similar model system studies. Imitating P450cam, the serine ligand was modeled as −OH[11]. We consider four spin states in total: **css** (closed-shell singlet), **oss** (open-shell singlet), triplet and quintet. The optimization of all open-shell singlet structures is carried out based on the initial guess of the triplet state, and then geometric optimization is performed according to the conjecture.

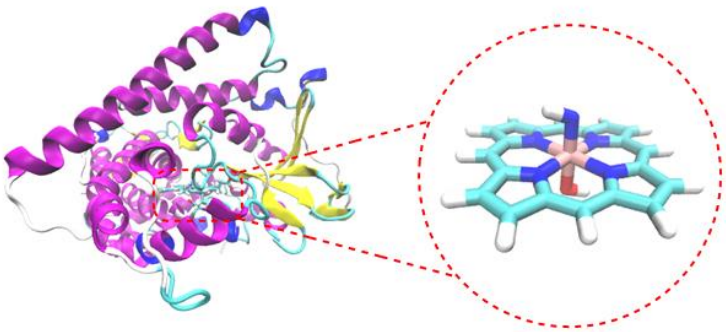

Fig. 2. Crystal structure of a variant (PDB ID: 5UCW) closely related to P411-B2 and simplified model used in our calculations

3 RESULTS AND DISCUSSION

3. 1 Geometry and electronic structure of the Fe(Por)(NH) species

In this section, the geometry and electronic structure of the Fe(Por)(NH) species are investigated. The optimized geometries of Fe(Por)(NH) in four different spin states (**css**, **oss**, triplet, and quintet) are presented in Fig. 3. The Fe(Por)(NH) species in the triplet state has the lowest energy among all spin states. The energy level of the open-shell state is only higher than that of the triplet ground state by 1.5 kcal/mol. In contrast, both the quintet state and the closed-shell singlet state lie on energy levels (9.3 and 10.1 kcal/mol, respectively) much higher than that of the triplet ground state. Thus, the primary amination reactions are mainly discussed with respect to the triplet and open-shell singlet state surfaces. The optimized geometries of the Fe(Por)(NH) species in these two states are shown in Fig. 3, where the lengths of Fe–N bonds are 1.83 (triplet state) and 1.87 Å (open-shell singlet state). Based on these values, the Fe–N bonds of Fe(Por)(NH) species in the triplet and open-shell states were determined to be single bonds. The spin densities of the Fe and N atoms in the triplet state are 1.00 and 1.03, respectively. In the open-shell singlet state, the spin density of Fe is 0.96, which is similar to that of its triplet state. However, the spin density of nitrogen in the open-shell singlet state is –0.99 and opposite of its spin density in the triplet state. These calculations indicate that one unit electron might transfer from nitrogen to $Fe^{(IV)}$, which would result in the formation of a $[(por)(–OH)–Fe^{III}–N^{\bullet-}–H]^-$ species with an $Fe^{(III)}$ metal center and a radical N atom.

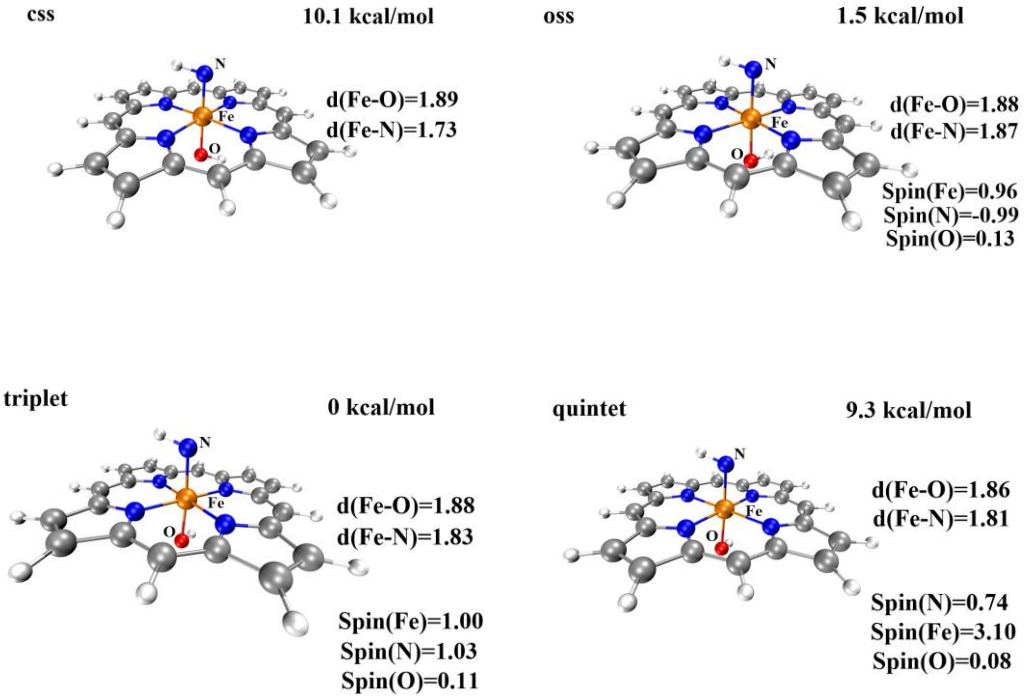

Fig. 3. Geometric optimization of the Fe(Por)(NH) species

To further understand the electronic configuration of the Fe(Por)(NH) species, we calculated its spin-natural orbitals (SNOs). We found that the triplet state contains two single-occupied orbitals, namely π^*_{xz} and π^*_{yz} (Fig. 4). The π^*_{xz} orbital is composed of the d_{xz} orbitals of Fe atom and the p_x orbitals of the nitrogen atom and mainly corresponds to the d orbital of Fe atom. The π^*_{yz} orbital is composed of the d_{yz} orbitals of the Fe atom and the p_y orbitals of the nitrogen atom and mainly corresponds to the p orbital of N atom. Furthermore, we used orbital composition analysis with the Mulliken partition to count the contributions of Fe and N atoms in the single-occupied SNOs. The calculations showed that the π^*_{yz} orbital (Orb. 2) contributions of the Fe and nitrogen atoms were approximately 28.8% and 66.4%, respectively, which implies that the unpaired electron preferred to occupy the p_y orbital of the nitrogen atom. Therefore, it would be possible for one unit electron to transfer from the N to the Fe atom, which indicates that a

resonance structure of the reactants exists; namely, [(por)(–OH)–Fe^{III}–$N^{\bullet-}$–H]$^-$ ↔ [(por)(–OH)–Fe^{IV}–N^{2-}–H]$^-$. For the open-shell singlet state, the Mulliken partition results show that the contributions of the Fe and N atoms in the π^*_{yz} orbital (Orb. 2) were approximately 1.03% and 95.1%, respectively. This result indicates that the unpaired electron is mainly located on the p_y orbital of the nitrogen atom. However, the biggest difference between the open-shell singlet and triplet states is the single-occupied orbital π^*_{yz}, which bears two spin-opposite electrons. The open-shell singlet state exhibits antiferromagnetic coupling between the π^*_{yz} orbital which possesses N radical character and the π^*_{xz} orbital which owns unpaired electrons on the d_{xz} orbitals of Fe. In contrast, the triplet state exhibited ferromagnetic coupling. Thus, the triplet and open-shell singlet states of Fe(Por)(NH) species are degenerate. Thus, the active structure of the P411 enzyme might exhibit resonance; namely, [(por)(–OH)–Fe^{III}–$N^{\bullet-}$–H]$^-$ ↔ [(por)(–OH)–Fe^{IV}–N^{2-}–H]$^-$.

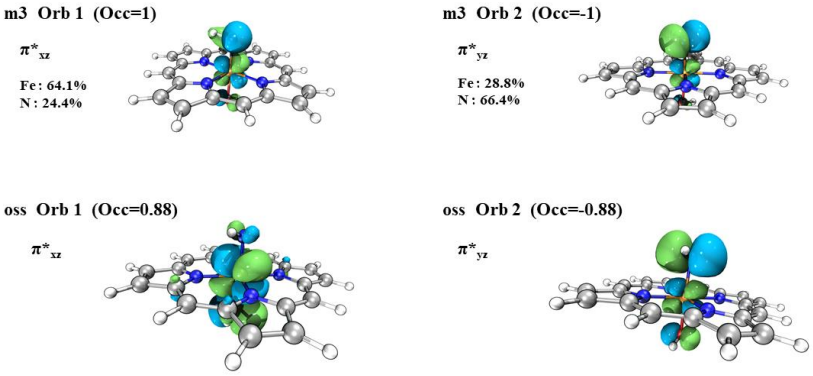

Fig. 4. Orbital composition analysis with Mulliken partition of the open-shell singletand triplet states of the Fe(Por)(NH) species

3. 2 Primary amination of the C(sp^3)−H bond of tetrahydronaphthalene

The amination of the C–H bond of **1** (reaction 1 in Scheme 1) catalyzed by the Fe(Por)(NH) species was then investigated. The optimized geometries of RC_1 in four different spin states (**css**, **oss**, triplet, and quintet) are shown in Fig. 5. The amination of the C(sp^3)−H bond of **1** consists of two main reaction steps: hydrogen-atom abstraction and radical recombination. Hydrogen atom H1 of substrate **1** is the target of the N atom of Fe(Por)(NH) for the abstraction process, and the distance between these two atoms is 3.04 Å. The process of this N atom abstracting H1 was investigated by scanning the energy profile during the acceptance of H1 by the N atom. The calculations indicate that the H1-atom abstraction must tackle a low energy barrier of only 7.1 kcal/mol to reach the transition state of $^3TS_1$, where the N–H1 distance decreases to 1.31 Å. As shown in Fig. 7, the single-occupied π^*_{yz} orbital of $^3RC_1$ is mainly distributed on the *p* orbital of the N atom, which is generally perpendicular to the Fe–N bond and coplanar with the N−H1−C1 plane. As a result, along with the coordination of N−H1 within the H-abstraction process, the radical orbital of the N atom could effectively overlap with the orbital of the C1−H1 bond, which could promote the H-abstraction of $^3RC_1$. Moreover, on the open-shell single state surface, the Fe(Por)(NH) species could undergo a similar H-abstraction process to that of the triplet ground state, except with a slightly higher energy for each structure.

Upon completion of the H-abstraction process, the radical intermediate ($^3IM_{1\text{-}1}$) of the [(por)(–OH)–Fe–NH_2]$^-$ species is generated. The optimized geometry of $IM_{1\text{-}1}$ revealed that the intermediate comprises a coordinated NH_2 group and a radial substrate within the cage (Fig. 6). The spin densities of the Fe, N, and C1 atoms changed from 1.04, 0.97, and 0.0 for RC_1 to 0.93, 0.08, and 0.71 for $IM_{1\text{-}1}$, respectively. The changes in the spin densities of these atoms from RC_1 to $IM_{1\text{-}1}$ indicate that spin-down electron transfers from the C−H1 σ orbital to the N *p* orbital upon the generation of $^3IM_{1\text{-}1}$ via the H1-atom abstraction process. Subsequently, the radical substrate and Fe(Por)(NH) species in the well-caged should undergo a so-called rebound reaction, which involves the amination of the radical substrate to generate the product. By scanning the energy profile of the process by which the distance between N and C1 along the rebound reaction coordination was shortened, the rebound reaction needed to conquer an energy barrier of only 0.6 kcal/mol to generate the product. Therefore, the H-abstraction is the rate-limiting step of the amination of C(sp^3)−H bond of substrate **1**. Additionally, this amination process involving open-shell singlet state surface is

similar to that involving the triplet ground state, which results in only slightly different energies for each produced structure. The potential energy surface of this reaction is shown in Fig.8.

We also considered another reaction site for the amina tion of C(sp^3)−H bonds, which resulted in a similar reaction process to those presented in the Supporting Information (Fig. S1).

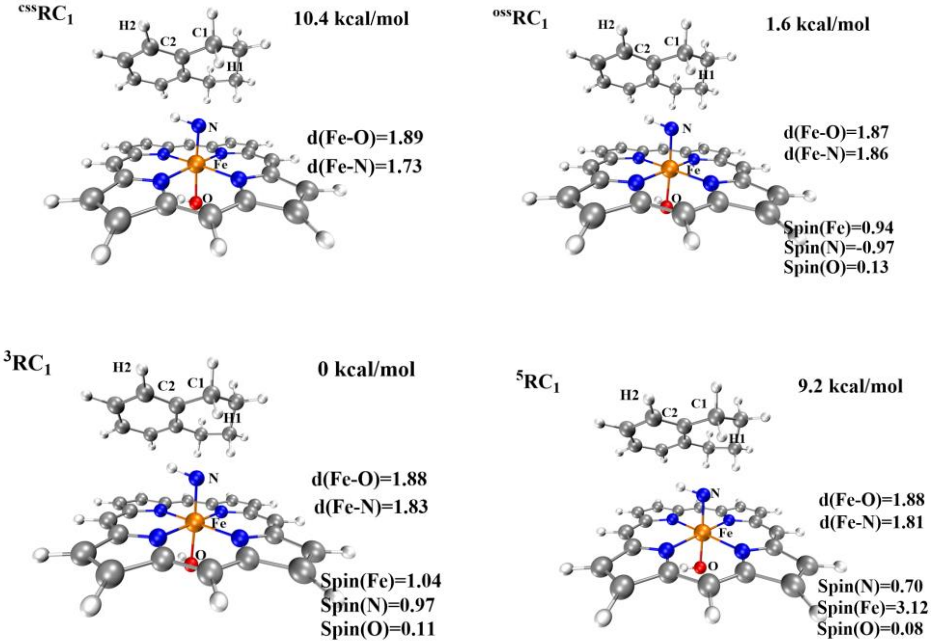

Fig. 5. Geometric optimization of the reactant structure

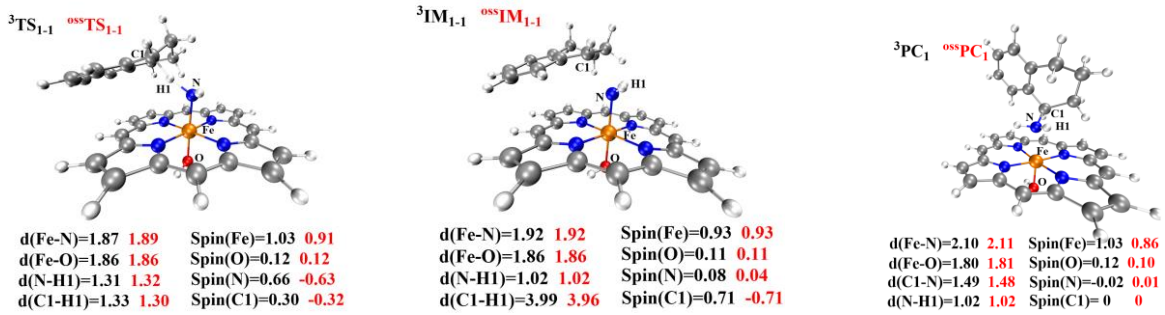

Fig. 6. Optimized structures of TS, IM and PC. Some important bond lengths and spin densities for the open-shell singlet and triplet states are listed. All distances are given in angstroms

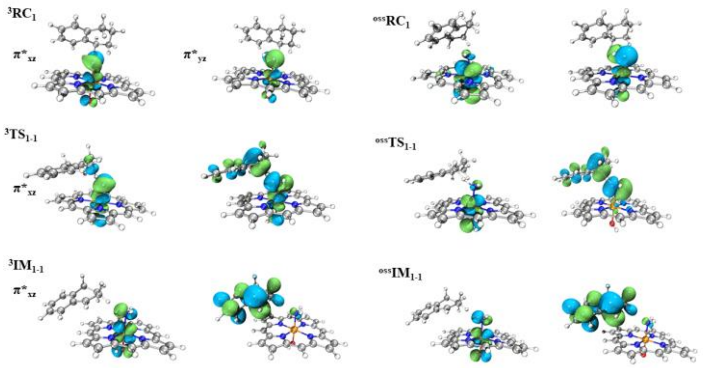

Fig. 7. Spin-natural orbitals (SNOs) of the open-shell singlet state and triplet state RC_1, TS_{1-1}, and IM_{1-1}. All orbitals were computed at the BS2 level of theory and are shown with their occupancies

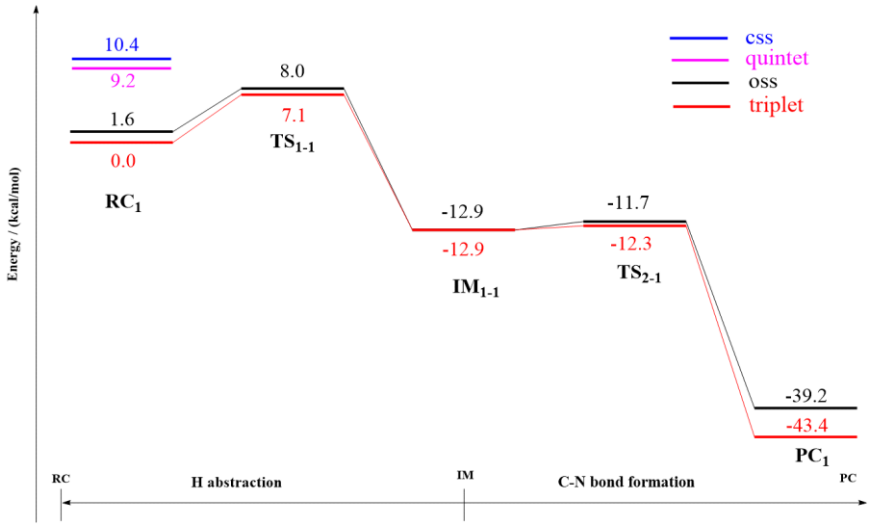

Fig. 8. Potential energy surface for C(sp^3)-H primary amination

Furthermore, according to the experimental result of Arnold's work[32], the product of C(sp^2)−H amination by the P411 enzyme can also be detected in negligible amounts. Thus, we also studied the primary amination of the C(sp^2)−H bonds of substrate **1**. Since benzene C(sp^2)−H bonds are very stable, the direct abstraction of their H atoms is very difficult. We calculated that an energy barrier greater than 30 kcal/mol would need to be overcome to accomplish this (Supporting Information, Fig. S2). Therefore, we investigated another possible reaction pathway for this C(sp^2)−H amination reaction involving the assistance of the porphyrin ligand (Fig. 9). Firstly, the N atom directly attacks the C2 atom to form a bridged imine group (energy barrier = 13.9 kcal/mol) to generate $IM_{1\text{-}2}$. Subsequently, the H2 atom of C(sp^2)–H bond is abstracted by the coordinated nitrogen. The energy barrier that must be overcome was calculated as 15.1 kcal/mol, which is lower than the energy barrier that must be overcome for the nitrogen to directly abstract the H2 atom (30.6 kcal/mol). Finally, the generated $IM_{2\text{-}2}$ undergoes a rebound reaction with fewer energy barriers and releases the product. Compared with the reaction pathway of C(sp^3)−H amination, the reaction of C(sp^2)−H amination requires a much higher energy barrier to be conquered than that required by the C(sp^3)−H bond amination. These reaction mechanism studies revealed that the H-abstraction is the rate-determining step, and that the P411 enzyme favorably catalyzes the primary amination of the C(sp^3)−H bond of tetrahydronaphthalene.

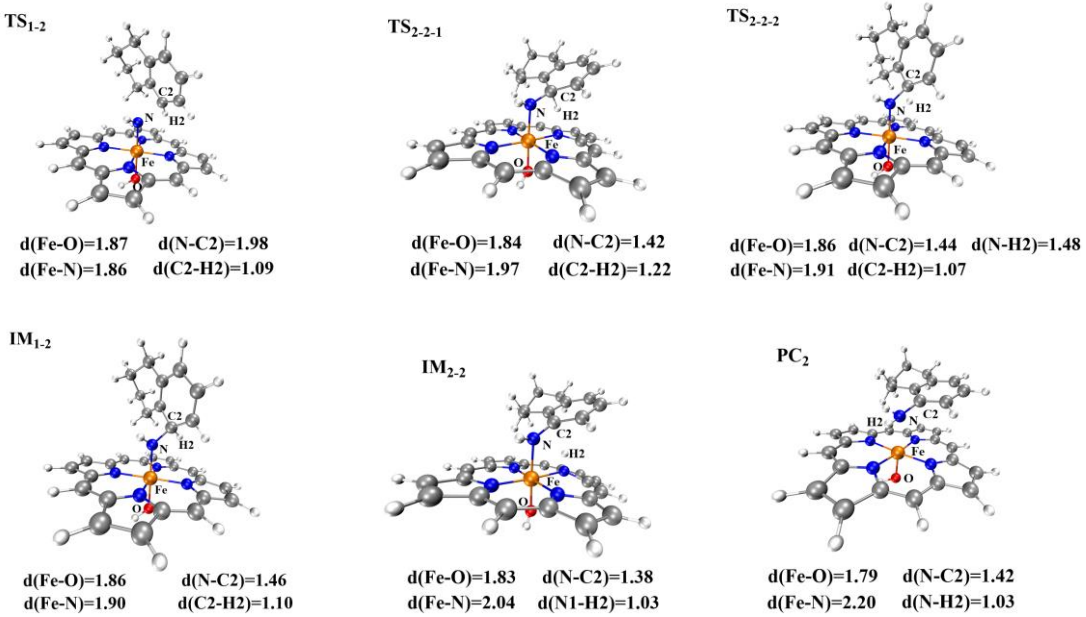

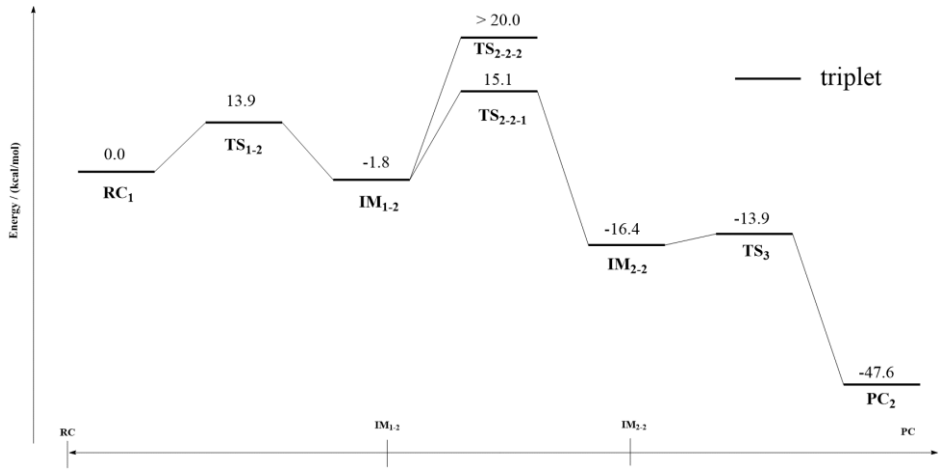

Fig. 9. Another possible reaction mechanism of C(sp^2)−H bond amination

3. 3 Regioselectivity of the primary amination of C(sp^3)−H bonds catalyzed by the P411 enzyme

We then investigated the regioselectivity of P411-enzyme-catalyzed primary amination of different C(sp^3)−H bonds (primary and secondary bonds) of 1-(3-methylphenyl) ethane (substrate **2** in Scheme 1). The optimized geometries of RC_2 when loading substrate **2** in four different spin states (css, oss, triplet, and quintet) are shown in Fig. 10. As discussed in the previous section, the active site of the triplet ground state and open-shell singlet state of RC_2 have the following resonance: $[(por)(–OH)\ Fe^{IV}–N^{2-}–H]^- \leftrightarrow [(por)(–OH)–Fe^{III}–N^{\bullet-}–H]^-$. This resonance can activate the C(sp^3)−H bond of substrate **2** (Scheme 1). Fig. 11 shows images of the potential energy surfaces of the aminations of primary and secondary C(sp^3)−H bonds that take place on the open-shell singlet state and triplet state surfaces, respectively.

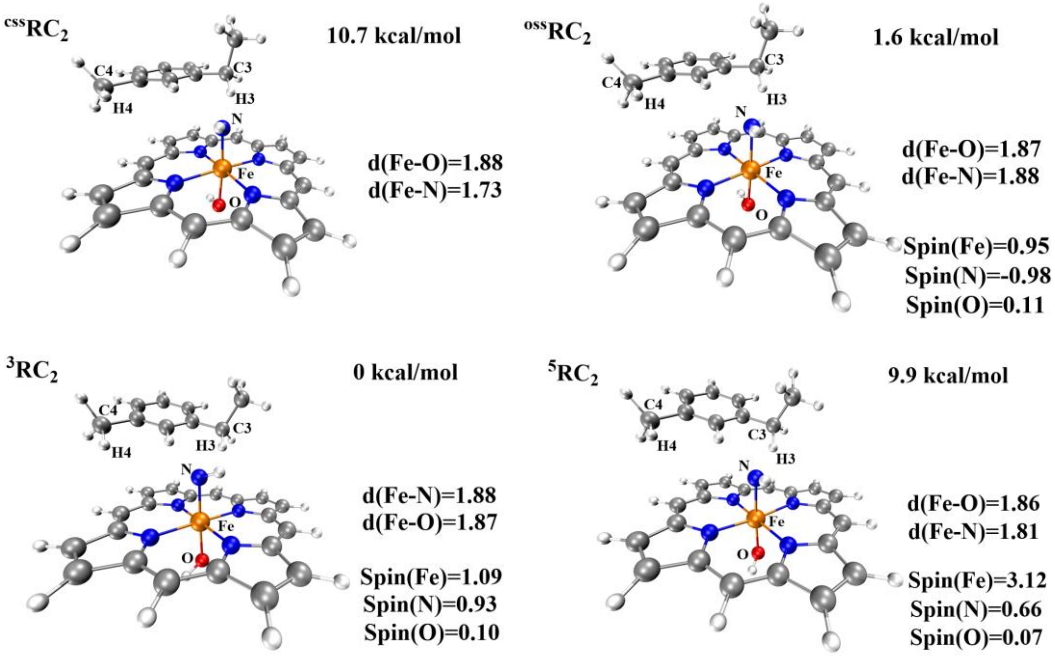

Fig. 10. Geometric optimization of the reactant structure

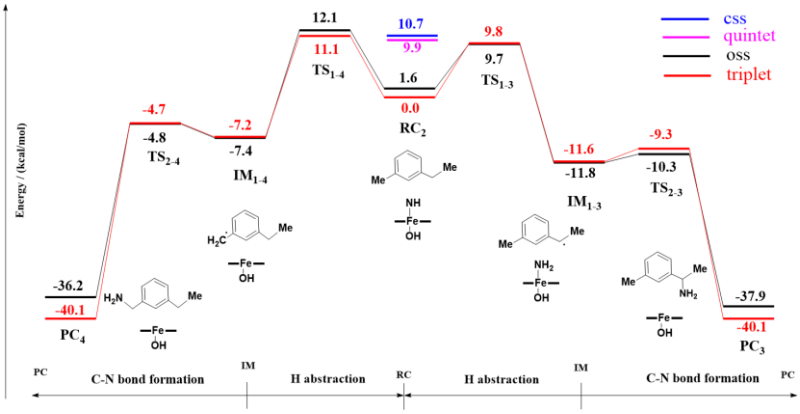

Fig. 11. Potential energy surfaces for the primary aminations of primary (left side of central axis) and secondary (right side of central axis) C(sp^3)−H bonds

The primary amination of the C(sp^3)−H bonds of the Fe(Por)(NH) species should undergo two main reaction steps: H-abstraction and radical recombination. The process by which Fe(Por)(NH) abstracts the H4 atom of **2** was investigated by scanning the energy profile of the N atom as it accepts the H4 atom. The calculations suggested that the abstraction of H4 requires an energy barrier of 11.1 kcal/mol at the triplet state (12.1 kcal/mol at the open-shell single state) to be overcome to generate the radical intermediate of $^3IM_{1-4}$. Finally, in $^3IM_{1-4}$, the coordinated NH_2 group would recombine with the radical C4 atom with only a slight barrier of 2.5 kcal/mol (2.6 kcal/mol in open-shell singlet) to overcome. In contrast, the H-abstraction step of the primary amination of the secondary C(sp^3)−H bonds requires an energy barrier of 9.8 kcal/mol (9.7 kcal/mol in open-shell singlet) to be conquered, which is lower than the barrier that must be overcome for the amination of the primary C(sp^3)−H bonds. Moreover, the generated radical intermediate IM_{1-3} has an energy level of −11.6 kcal/mol (−11.8 kcal/mol in open-shell singlet), which is lower than that of IM_{1-4} (−7.2 kcal/mol; −7.4 kcal/mol in open-shell singlet). These calculations reveal that the secondary C(sp^3)−H bond is more easily activated by the Fe(Por)(NH) species than the primary C(sp^3)−H bond. Subsequently, the rebound reaction must overcome only a slight barrier to achieve the rebound of the NH_2 group to the radical substrate **2** in IM_{1-4}, resulting in the formation of the product. Additionally, the reaction pathway of Fe(Por)(NH)-catalyzed amination of the secondary C(sp^3)−H bonds in the open-shell single state is similar to that in the triplet ground state, with only slightly different energies for each structure. Therefore, the P411 enzyme is energetically favored for aminations of secondary C(sp^3)−H bonds.

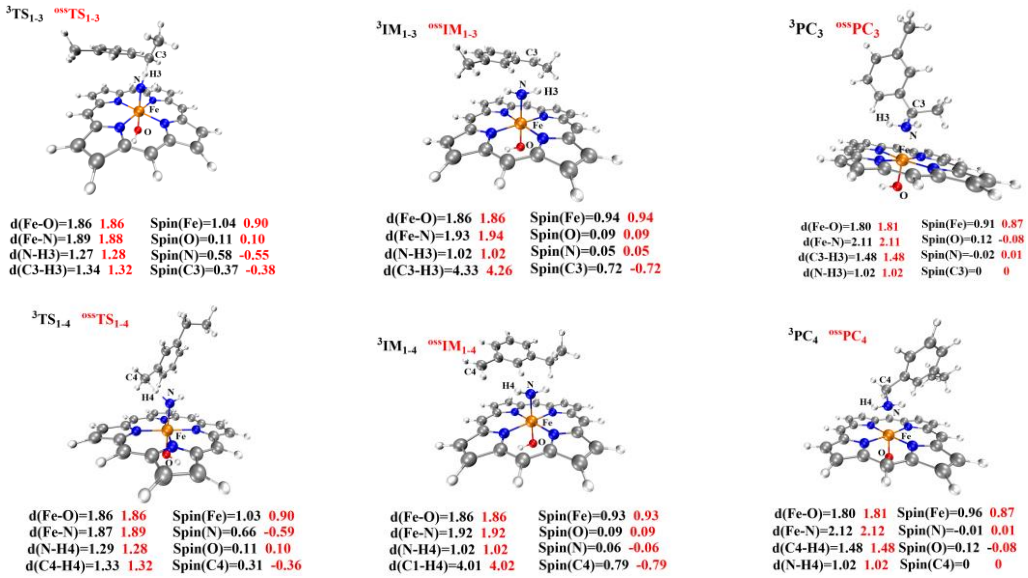

Fig. 12. Geometric optimization of the structures of TS, IM and PC of primary and secondary C(sp^3)−H bonds. Some important bond lengths and spin densities for the open-shell singlet and triplet states are provided. All distances are given in angstroms

According to our calculations, the H-abstraction step is the rate-determining step of the reaction pathway of the primary amination of C(sp^3)−H bonds, which involves an electron transferring from the reactive moiety of the substrate to the Fe(Por)(NH) species. Thus, it can be expected that if the reactive moiety of the substrate is a better electron donor, the barrier of H-abstraction toward that moiety would be decreased. To further understand the reason for the preferred amination of secondary C(sp^3)−H bonds, we investigated the SNOs via orbital composition analysis with Mulliken partitions of the primary and secondary C−H moieties of the substrate. As shown in Fig. 13, the single-occupied SNOs of TS_{1-3} and TS_{1-4} represent the orbitals interacting when the N atom of Fe(Por)(NH) attacks the primary and secondary C(sp^3)−H moieties, respectively of the substrate. For TS_{1-4}, the C4-atom (primary carbon) contribution to the transfer process was 20.3%, while the contributions of N and Fe atoms of the Fe–N center were 43.6% and 21.5%, respectively. For the single-occupied SNOs of TS_{1-3}, the contribution of the C3 atom (secondary carbon) of the substrate to the transfer process was 12.9%, while those of the N and Fe atoms of the Fe–N center were 34.0% and 42.6%, respectively. Upon comparing these results, it is obvious that the contribution of carbon atoms to the single-occupied SNOs of the transition state at the secondary site is lower than that at the primary site. Meanwhile, the higher contribution (42.6～21.5%) of the Fe atom of the Fe–N active center also indicates that the secondary C−H bonds may be more easily reactivated by the Fe(Por)(NH) species than the primary bonds, and the barrier of C−H bond activation should be reduced. This distinguishes the contribution of TS_{1-3} and TS_{1-4} to the single-occupied SNOs, indicating that the secondary C(sp^3)−H moiety of the substrate exhibits a stronger electron-donor ability than that of the primary C(sp^3)−H moiety. As a result, the Fe(Por)(NH) species abstracts the H3 atom from the secondary site of the substrate, which is promoted by the stronger electron-donor ability of the primary site. Therefore, the Fe(Por)(NH) species preferentially catalyzes the primary amination of secondary C(sp^3)−H bonds.

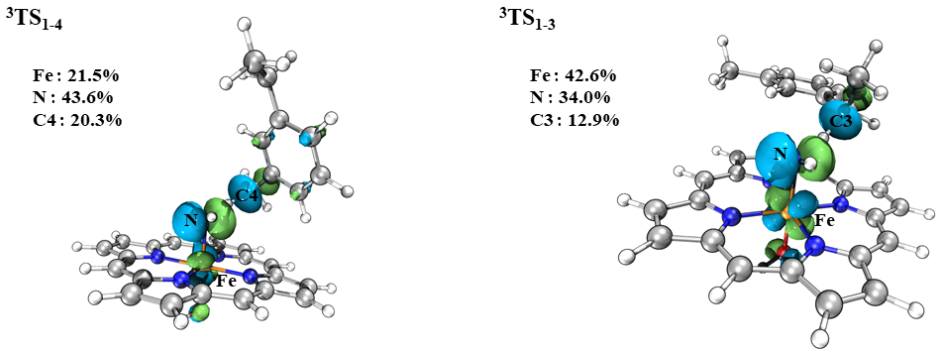

Fig. 13. Transition-state single-occupied SNOs and the contribution of selected atoms

4 CONCLUSION

In this work, we employed the DFT method to study the electronic structure of the active center of the cytochrome P411 enzyme and the primary amination of C−H bonds catalyzed by its Fe(Por)(NH) species. The calculated spin densities and SNOs indicated the existence of resonance in the reactants; namely, [(por)(–OH) Fe^{IV}–N^{2-}–H]$^-$ ↔ [(por)-(–OH)Fe^{III}–$N^{\bullet-}$–H]$^-$. Then, we explored the reactivity of this Fe(Por)(NH) species and revealed the reaction mechanism through which it aminates the C(sp^3)−H bonds of substrate tetrahydronaphthalene. The calculated reaction pathway occurring on the triplet ground state surface indicates that the H-abstraction is the rate-determining step of the primary amination. We also found that the energy barrier to be overcome for the subsequent NH_2-group rebound reaction to proceed is lower than that of H-abstraction step.

Furthermore, the regioselectivity of Fe(Por)(NH)-catalyzed primary amination of different C(sp^3)−H bonds (primary and secondary bonds) was investigated using substrate 1-(3-methylphenyl) ethan. Distinguishing the orbital contribution of single-occupied SNOs in the transition state indicated that the secondary C(sp^3)−H moiety of the substrate has a stronger electronic donor ability than that of the primary C(sp^3)−H moiety. Therefore, the secondary site of the substrate would be favored for activation by the P411 enzyme. The calculation of the above reactivity and selectivity of the P411 enzyme can provide useful ideas and

information for understanding the properties and selectivity of the C−H/C−N bond-activation reactions it catalyzes, as well as those catalyzed by similar enzymes. Our results can also be used for developing and synthesizing new, related catalysts.

REFERENCES

(1) Bräse, S. Amino group chemistry: from synthesis to the life sciences. *ChemBioChem.* **2008**, 9, 15093−1509.

(2) Davies, H. M. L.; Morton, D. Collective approach to advancing C−H functionalization. *ACS Central Sci.* **2017**, 3, 936−943.

(3) Yang, Y.; Cho, I.; Qi, X.; Liu, P.; Arnold, F. H. An enzymatic platform for the asymmetric amination of primary, secondary and tertiary C(*sp*(3))−H bonds. *Nat. Chem.* **2019**, 11, 987−993.

(4) Hennessy, E. T.; Betley, T. A. Complex N-heterocycle synthesis via iron-catalyzed, direct C−H bond amination. *Science* **2013**, 340, 591−595.

(5) Paudyal, M. P.; Adebesin, A. M.; Burt, S. R.; Ess, D. H.; Ma, Z.; Kurti, L.; Falck, J. R. Dirhodium-catalyzed C−H arene amination using hydroxylamines. *Science* **2016**, 353, 1144−1147.

(6) Gross, T.; Seayad, A. M.; Ahmad, M.; Beller, M. Synthesis of primary amines: first homogeneously catalyzed reductive amination with ammonia. *Org. Lett.* **2002**, 4, 2055−2058.

(7) Hartwig, J. F. Evolution of a fourth generation catalyst for the amination and thioetherification of aryl halides. *Accounts Chem. Res.* **2008**, 41, 1534−1544.

(8) Surry, D. S.; Buchwald, S. L. Biaryl phosphane ligands in palladium-catalyzed amination. *Angew. Chem., Int. Ed Chem.* **2008**, 47, 6338−6361.

(9) Dydio, P.; Key, H. M.; Hayashi, H.; Clark, D. S.; Hartwig, J. F. Chemoselective, enzymatic C−H bond amination catalyzed by a cytochrome P450 containing an Ir(Me)-PIX cofactor. *J. Am. Chem. Soc.* **2017**, 139, 1750−1753.

(10) Hyster, T. K.; Farwell, C. C.; Buller, A. R.; McIntosh, J. A.; Arnold, F. H. Enzyme-controlled nitrogen-atom transfer enables regiodivergent C−H amination. *J. Am. Chem. Soc.* **2014**, 136, 15505−15508.

(11) McIntosh, J. A.; Coelho, P. S.; Farwell, C. C.; Wang, Z. J.; Lewis, J. C.; Brown, T. R.; Arnold, F. H. Enantioselective intramolecular C−H amination catalyzed by engineered cytochrome P450 enzymes in vitro and in vivo. *Angew. Chem., Int. Edit.* **2013**, 52, 9309−9312.

(12) Singh, R.; Bordeaux, M.; Fasan, R. P450-Catalyzed intramolecular sp^3 C−H amination with arylsulfonyl azide substrates. *ACS Catal.* **2014**, 4, 546−552.

(13) Singh, R.; Kolev, J. N.; Sutera, P. A.; Fasan, R. Enzymatic C(sp^3)−H amination: P450-catalyzed conversion of carbonazidates into oxazolidinones. *ACS Catal.* **2015**, 5, 1685−1691.

(14) Zalatan, D. N.; Du Bois, J. Metal-catalyzed oxidations of C−H to C−N bonds. C−H activation. *Topics in Current Chemistry−Series.* **2010**, 292, 347−378.

(15) Davies, H. M. L.; Manning, J. R. Catalytic C−H functionalization by metal carbenoid and nitrenoid insertion. *Nature* **2008**, 451, 417−424.

(16) Collet, F.; Lescot, C.; Dauban, P. Catalytic C−H amination: the stereoselectivity issue. *Chem. Soc. Rev.* **2011**, 40, 1926−1936.

(17) Jeffrey, J. L.; Sarpong, R. Intramolecular C(sp^3)−H amination. *Chem. Sci.* **2013**, 4, 4092−4106.

(18) Hartwig, J. F. Evolution of C−H bond functionalization from methane to methodology. *J. Am. Chem. Soc.* **2016**, 138, 2−24.

(19) Godula, K.; Sames, D. C−H bond functionalization in complex organic synthesis. *Science* **2006**, 312, 67−72.

(20) Yamaguchi, J.; Yamaguchi, A. D.; Itami, K. C−H mond functionalization: emerging synthetic tools for natural products and pharmaceuticals. *Angew. Chem., Int. Edit.* **2012**, 51, 8960−9009.

(21) Romero, N. A.; Margrey, K. A.; Tay, N. E. Nicewicz, D. A. Site-selective arene C−H amination *via* photoredox catalysis. *Science* **2015**, 349, 1326−1330.

(22) Zheng, Y. W.; Chen, B.; Ye, P.; Feng, K.; Wang, W.; Meng, Q. Y.; Wu, L. Z.; Tung, C. H. Photocatalytic hydrogen-evolution cross-couplings: benzene C−H amination and hydroxylation. *J. Am. Chem. Soc.* **2016**, 138, 10080−10083.

(23) Morofuji, T.; Shimizu, A.; Yoshida, J. I. Electrochemical C−H amination: synthesis of aromatic primary amines via N-arylpyridinium ions. *J. Am. Chem. Soc.* **2013**, 135, 5000−5003.

(24) Peng, J.; Chen, M.; Xie, Z.; Luo, S.; Zhu, Q. Copper-mediated C(sp^2)-H amination using TMSN3 as a nitrogen source: redox-neutral access to primary anilines. *Org. Chem. Front.* **2014**, 1, 777−781.

(25) Tezuka, N.; Shirnojo, K.; Hirano, K.; Komagawa, S.; Yoshida, K.; Wang, C.; Miyamoto, K.; Saito, T.; Takita, R.; Uchiyama, M. Direct hydroxylation and amination of arenes via deprotonative cupration. *J. Am. Chem. Soc.* **2016**, 138, 9166−9171.

(26) Legnani, L.; Cerai, G. P.; Morandi, B. Direct and practical synthesis of primary anilines through iron-catalyzed C–H bond amination. *ACS Catal.* **2016**, 6, 8162−8165.

(27) Liu, J.; Wu, K.; Shen, T.; Liang, Y.; Zou, M.; Zhu, Y.; Li, X.; Li, X.; Jiao, N. Fe-catalyzed amination of (hetero)arenes with a redox-active aminating reagent under mild conditions. *Chem. Eur. J.* **2017**, 23, 563−567.

(28) Kim, H.; Heo, J.; Kim, J.; Baik, M. H.; Chang, S. Copper-mediated amination of aryl C−H bonds with the direct use of aqueous ammonia via a disproportionation pathway. *J. Am. Chem. Soc.* **2018**, 140, 14350−14356.

(29) Anugu, R. R.; Munnuri, S.; Falck, J. R. Picolinate-directed arene meta-C–H amination *via* $FeCl_3$ catalysis. *J. Am. Chem. Soc.* **2020**, 142, 5266−5271.

(30) Shaik, S.; Cohen, S.; Wang, Y.; Chen, H.; Kumar, D.; Thiel, W. P450 enzymes: their structure, reactivity, and selectivity-modeled by QM/MM calculations. *Chem. Rev.* **2010**, 110, 949−1017.

(31) Hyster, T. K.; Arnold, F. H. P450BM3−axial mutations: a gateway to non-natural reactivity. *Isr. J. Chem.* **2015**, 55, 14−20.

(32) Jia, Z. J.; Gao, S.; Arnold, F. H. Enzymatic primary amination of benzylic and allylic C(sp^3)–H bonds. *J. Am. Chem. Soc.* **2020**, 142, 10279−10283.

(33) Coelho, P. S.; Wang, Z. J.; Ener, M. E.; Baril, S. A.; Kannan, A.; Arnold, F. H.; Brustad, E. M. A serine-substituted P450 catalyzes highly efficient carbene transfer to olefins in vivo. *Nat. Chem. Biol.* **2013**, 9, 485−U33.

(34) Wang, J.; Gao, H.; Yang, L.; Gao, Y. Q. Role of engineered iron-haem enzyme in reactivity and stereoselectivity of intermolecular benzylic C−H bond amination. *ACS Catal.* **2020**, 10, 5318−5327.

(35) Li, P.; Merz, K. M. Jr. MCPB.py: a python based metal center parameter builder. *J. Chem. Inf. Model.* **2016**, 56, 599−604.

(36) Wang, J. M.; Wolf, R. M.; Caldwell, J. W.; Kollman, P. A.; Case, D. A. Development and testing of a general amber force field. *J. Comput. Chem.* **2004**, 25, 1157−1174.

(37) Li, H.; Robertson, A. D.; Jensen, J. H. Very fast empirical prediction and rationalization of protein pKa values. *Proteins* **2005**, 61, 704−721.

(38) Humphrey, W.; Dalke, A.; Schulten, K. VMD: visual molecular dynamics. *J. Mol. Graph.* **1996**, 14, 33−38.

(39) Izaguirre, J. A.; Catarello, D. P.; Wozniak, J. M.; Skeel, R. D. Langevin stabilization of molecular dynamics. *J. Chem. Phys.* **2001**, 114, 2090−2098.

(40) Berendsen, H. J. C.; Postma, J. P. M.; Vangunsteren, W. F.; Dinola, A.; Haak, J. R. Molecular-dynamics with coupling to an external bath. *J. Chem. Phys.* **1984**, 81, 3684−3690.

(41) Shahrokh, K.; Orendt, A.; Yost, G. S.; Cheatham, T. E. III. Quantum mechanically derived AMBER-compatible heme parameters for various states of the cytochrome P450 catalytic cycle. *J. Comput. Chem.* **2012**, 33, 119−133.

(42) Neese, F. The ORCA program system. *Wiley Interdiscip. Rev. Comput. Mol. Sci.* **2012**, 2, 73−78.

(43) Ahmad, F.; Alam, M. J.; Alam, M.; Azaz, S.; Parveen, M.; Park, S.; Ahmad, S. Synthesis, spectroscopic, computational (DFT/B3LYP), AChE inhibition and antioxidant studies of imidazole derivative. *J. Mol. Struct.* **2018**, 1151, 327−342.

(44) Marenich, A. V.; Cramer, C. J.; Truhlar, D. G. Universal solvation model based on solute electron density and on a continuum model of the solvent defined by the bulk dielectric constant and atomic surface tensions. *J. Phys. Chem. B* **2009**, 113, 6378−6396.

(45) Li, X.; Dong, L.; Liu, Y. Theoretical study of iron porphyrin nitrene: formation mechanism, electronic nature, and intermolecular C−H Amination. *Inorg. Chem.* **2020**, 59, 1622−1632.